P2.20 HYPERSPECTRAL INFRARED ICE CLOUD PROPERTY RETRIEVAL DEMONSTRATION – THEORETICAL AND CASE STUDY ANALYSIS

Hung-Lung Huang[1], Ping Yang[2], He-Li Wei[2], Bryan A. Baum[3], Yongxiang Hu[3], Paolo Antonelli[1], Steven A. Ackerman[1]

[1] Cooperative Institute for Meteorological Satellite Studies, University of Wisconsin-Madison,
[2] Texas A&M University, Department of Atmospheric Sciences
[3] NASA Langley Research Center

1. INTRODUCTION

Hyperspectral measurements of infrared radiance covering the range from 790 to 1250 wavenumbers contain information on the abundance, size and shape of ice crystals in ice clouds. Recent advances in cloud radiative transfer modeling, and in hyperspectral retrieval techniques, now allow for the possibility of deriving cloud optical thickness and effective particle size from such measurements. A significant climate study application of this new capability is assessing the impacts of cloud properties on the Earth's radiation budget through feedback mechanism and radiative forcing.

This paper reviews, briefly, 1) forward scattering and radiative transfer modeling, 2) single-scattering properties of ice clouds, 3) simulation of infrared cloudy radiances, 4) measurements effects of ice crystal habits, 5) impact of the assumption of Henyey-Greenstein phase function, 6) effect on cloud property retrieval of knowledge of surface and cloud temperature, and of atmospheric profile, and 7) cloud property retrieval approach. Retrieval results from SUCCESS and FIRE-ACE field measurements are also presented as case studies. An extension of this manuscript is under preparation for publication.

2. SINGLE SCATTERING PROPERTIES OF CIE CLOUDS AND SIMULATIONS OF CLOUDY RADIANCES

In this study, we use droxtals to represent small particles with size up to 32 μm in terms of maximum dimension, and hexagonal columns to represent larger particles. A number of investigators assumed that ice crystals are hexagonal, which is a traditional non-spherical particle. Yang (Yang et al., 2001) explained the use of hexagonal ice crystals for infrared (IR) radiative calculations in cirrus clouds. Scattering and absorption properties of droxtals and small hexagonal ice crystals are calculated using the finite-difference time-domain (FDTD) method (Yang and Liou, 1996).

Corresponding author address: Hung-Lung Allen Huang, Cooperative Institute for Meteorological Satellite Studies, University of Wisconsin-Madison, 1225 West Dayton Street, Madison, WI 53706. E-mail: allenh@ssec.wisc.edu

Figure 1 shows a comparison of the scattering phase functions at 1250 cm^{-1} for spherical, droxtal and hexagonal (with an aspect ratio of 1) ice crystal particles with the same maximum dimension of 10 μm. The phase function of the spherical particle was calculated from Lorenz-Mie theory using the computation code developed by *Wiscombe* (1980). As shown in figure 1, the scattering phase function is different for the three particle geometries in forward and backward directions. The forward scattering by droxtals is smaller than that by either hexagonal or spherical crystals because the volume of the droxtal is the smallest for the same maximum dimension. The positions of scattering sub-maximum are different for different shapes.
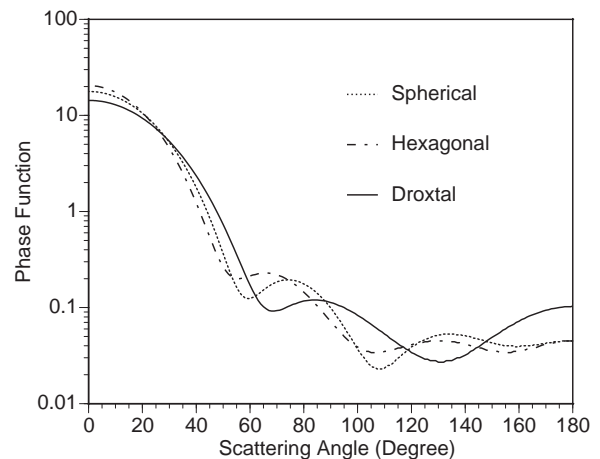

Fig. 1: Comparison of phase functions for droxtals, hexagonal columns, and spherical ice crystals with maximum dimension 10 μm at a wavenumber of 1250 cm^{-1} (wavelength 8.0 μm).

The calculations shown in figure 2 were performed using the parameterization scheme developed by *Yang et al.* (Yang et al., 2001) for the optical properties of ice crystals. The mean extinction efficiency of ice crystals depends strongly on wavenumber, particularly, for small particle sizes. The extinction minimum at 950 cm^{-1}, which becomes more pronounced with decreasing particle size, corresponds to the Christiansen band of ice (Arnott et al., 1995; Yang et al., 1997). For large particle sizes (D_e=50 or 80 μm) the spectral variation of the extinction efficiency is relatively smooth. The total

extinction efficiency of ice crystals (i.e., the sum of scattering and absorption effects) in the 1000–1250 cm^{-1} spectral region is nearly independent of effective particle size for large particles, a characteristic that is useful for the retrieval of ice cloud optical thickness.

The bulk absorption efficiency is related to the imaginary component of the refractive index of ice. In addition, the absorption of ice crystals depends on wavenumber and the effective particle size of the particles. The absorption efficiency varies with wavenumber in the 750–1000 cm^{-1} spectral region, particularly for small ice particles. This feature is useful for determining the effective size of ice crystals from high-resolution IR atmospheric spectral measurements. The asymmetry factor increases with effective particle size in the IR spectral region, implying that the scattering of the incident radiation by ice crystals is typically in the forward direction.
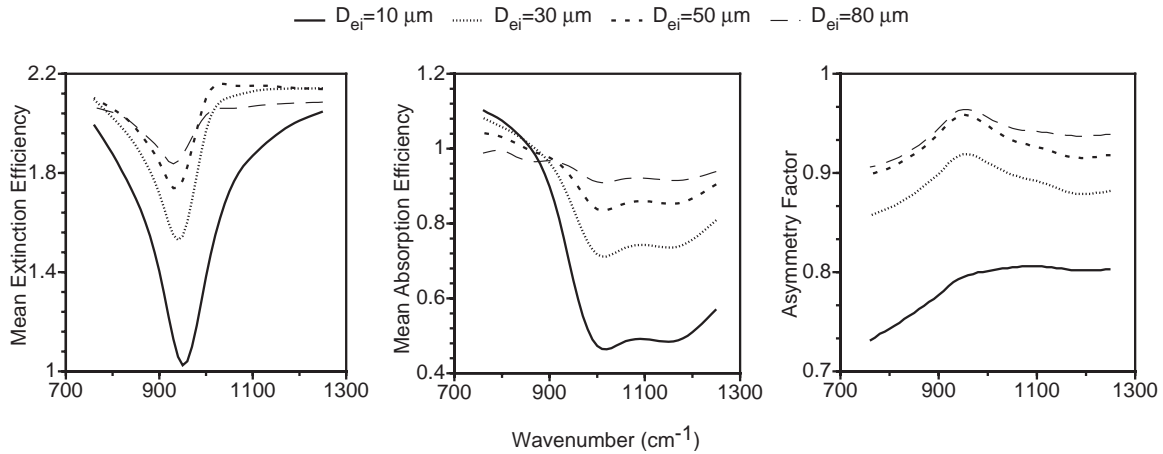

Fig. 2 Single-scattering properties of ice clouds for four effective particle sizes.

Clear-sky (non-cloudy) monochromatic atmospheric molecular absorption optical thicknesses are computed from a line-by-line (LBL) radiative transfer model originally developed by Chou and Kouvaris (1986). For the present application, the atmosphere is divided into one hundred layers between the surface and an altitude of 20 km. Rawinsonde profiles provide atmospheric temperature, pressure, density and water vapor; the spectral line parameters of atmospheric gases are from HITRAN 2000 (Rothman et al., 1998); and the Voigt line shape (Kielkopf, 1973) that accounts for both pressure and temperature broadening effects is used for computing the line absorption of atmospheric gas molecules. The continuum absorption of water vapor and other gases within 750–1250 cm^{-1} are calculated using the CKD-2.4 model (Tobin et al., 1999). To facilitate later comparisons with HIS (Revercomb, et al., 1988) data needed in the implementation of the retrieval technique, the monochromatic total optical thicknesses of atmospheric gases at every level are convolved with the instrumental response function.

The upwelling atmospheric radiative spectrum under cloudy conditions at the aircraft altitude (20 km) is then computed in terms of brightness temperature by combining the clear-sky optical thickness from the LBL code and the discrete ordinates method radiative transfer (DISORT) (Stamnes et al., 1988). Clouds are simulated by adding an optical thickness, single-scattering albedo, and scattering phase function into a model layer atmosphere. The DISORT method is used with 16 streams in the calculations. The spectral interval is 0.2cm^{-1}. The Legendre coefficients of the phase function of ice crystals are derived using an algorithm that properly accounts for the truncation of the strong forward peak (Hu et al., 2000)

3. SENSITIVITY STUDY AND ERROR ANALYSIS

Figure 3 illustrates the sensitivity of the upwelling brightness temperature spectrum to the ice cloud effective particle size.
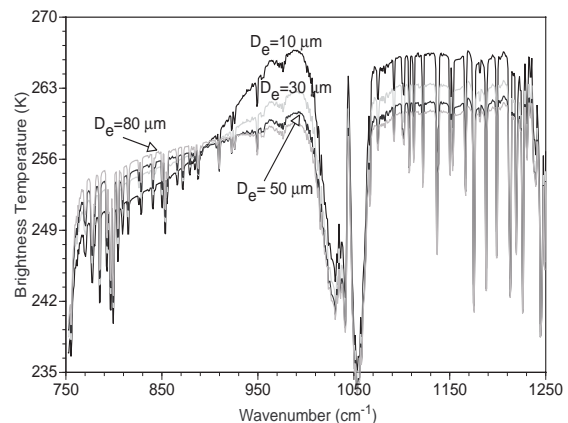

Fig. 3: Shown are the spectral brightness temperatures at the aircraft level (20km) as a function of wavenumber for four effective particle sizes (10, 30, 50, and 80 μm). The calculations assume the US standard atmospheric model, a surface skin temperature of 288.1 K, a cloud altitude of 10 km, and an optical thickness Tau=1.

The spectral brightness temperatures between atmospheric molecular absorption lines (i.e., the atmospheric windows) increase with wavenumber within the 760–1000cm^{-1} region due to the fact that the absorption of ice crystal particles decreases with wavenumber and the absorption is also size-dependent. The cirrus clouds with smaller effective sizes absorb more radiance from below in the region of small wavenumbers, leading to a stepper slope for cirrus clouds composed of small particles than for cirrus clouds composed of large particles. From the brightness temperature at atmospheric window wavenumbers, igoring the strong absorption wavenumbers to remove the absorption lines between 790–960 cm^{-1} and interpolating the brightness temperatures across the gaps, we notice that there is a marked sensitivity in the slope of the observed brightness temperature to the effective particle size (see Fig.3). This sensitivity, in which the slope in brightness temperature increases with decreasing particle size, forms the basis for the inference of effective particle size. We calculate the brightness temperature at the atmospheric windows in the 790–960 cm^{-1} region, and obtain the slope for a range of different effective particle sizes and values of optical thickness. As shown in figure. 4, the variation of the slope is most sensitive to particle size for small particles and optical thicknesses between 0.4 and 4. For example, for a cloud having an optical thickness of 1, the slope decreases from 9 K/μm to 2 K/μm as the effective particle size increases from 10 μm to 80 μm.
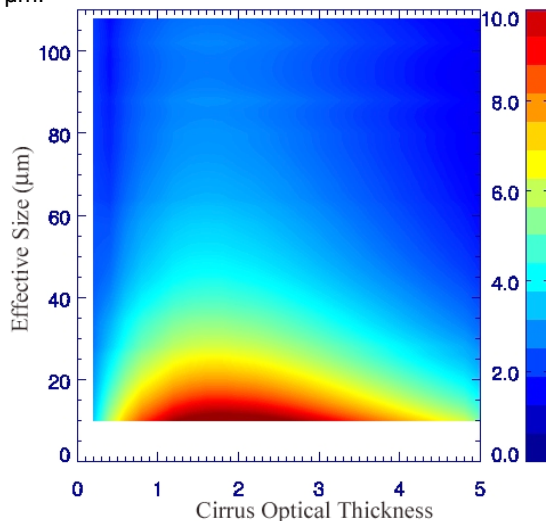

Fig. 4: Effect of optical thickness and particle size on the slope of the spectral brightness temperatures and wavenumber between 790–960 cm^{-1}.

Figure 5 shows simulated upwelling brightness temperature at a 20-km altitude for four values of optical thickness and a fixed effective particle size of 30 μm. The brightness temperature varies with wavenumber between 750–1000 cm^{-1} for small to moderate optical thicknesses. As shown in figure 5, the brightness temperature decreases more than 40 K

as the optical thickness increases from 0.5 to 5. For optically thick ice clouds (optical thickness larger than 5), the brightness temperature has less dependence on wavenumber.
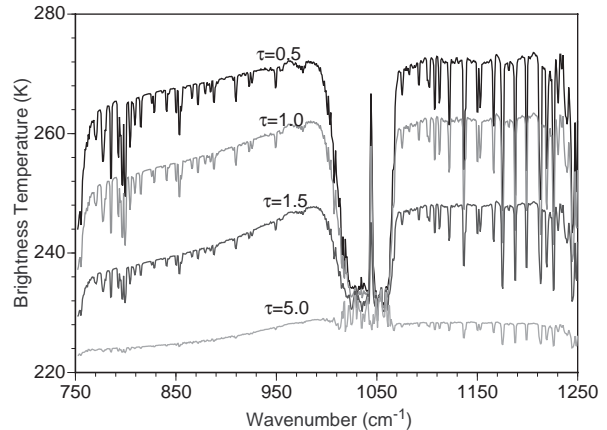

Fig. 5: The sensitivity of spectral brightness temperature to the cloud optical thickness. The assumed effective particle size is fixed at 30 μm.

The brightness temperature discretization in Fig. 4 is 0.5 K/μm. If we assume the minimum measurable temperature difference is 1 K, then the effective particle size cannot be accurately retrieved if the variation of brightness temperature difference between 950 and 790 cm^{-1} is less than 1 K due to the variation of the effective particle size. Further theoretical error analysis suggested that, for a threshold of 0.5 K/μm, the maximum retrievable effective size is no larger than 80 μm with an uncertainty of 10 μm. The uncertainty decreases to about 2 μm when the effective size is 10 μm. Similarly, the maximum retrievable optical thickness is approximately 8 with an uncertainty of 1. For the case of a visible optical thickness of 1, the uncertainty decreases to less than 0.1.

In the IR spectrum, the surface skin temperature, cloud temperature and atmospheric profile contributed significantly to the top of atmosphere radiance. Hence, in the remains of the section, we study the effects of uncertainties in surface and cloud temperature to retrieval results. We also investigate the variation of the sensitivity for different atmospheric profiles.

Cloud-top pressure or temperature may be inferred by methods such as the CO_2 slicing method (wylie and Menzel, 1999) or by the minimum local emissivity variance (MLEV) method (Huang et al., 2003). The MLEV algorithm uses a physical approach in which the local spectral variances of cloud emissivity are calculated for a number of assumed cloud pressures. The optimal cloud emissivity spectrum is that which has the minimum local emissivity variance among the retrieved emissivity spectra associated with different assumed cloud pressures. This technique is based on the observation that the absorption, reflection, and scattering processes of clouds exhibit relatively limited localized spectral emissivity structure in the

750–1250 cm^{-1} spectral region. Any retrieved cloud emissivity that exhibits spectral variation similar to that of carbon dioxide and water vapor absorption is indicative of an incorrect specification of cloud pressure level and its associated spectral emissivity. MLEV analysis shows that cloud pressure root mean square errors for a single layer cloud with effective cloud emissivity greater than 0.1 are ~30 hPa, ~10 hPa, and ~50 hPa, for high, middle, and low clouds, respectively.

Errors in the assigned cloud pressure and its corresponding temperature will affect the retrieval of optical thickness. Figure 6 shows the predicted error in the retrieved optical thickness as a function of cloud temperature error. The error of cloud temperature is assumed to be within ±7 K, corresponding to the variation of temperature at a cloud altitude of 10±1 km. A lower-than-actual cloud temperature will result in an overestimate of the optical thickness, while a higher-than-actual cloud temperature will lead to an underestimate of optical thickness. The impact of the cloud temperature error is more pronounced for optically thick ice clouds than for optically thin ice clouds. Generally, the error in the retrieved optical thickness is less than 10% if the cloud temperature is within ±5 K of the true temperature and the cloud optical thickness is less than 2.
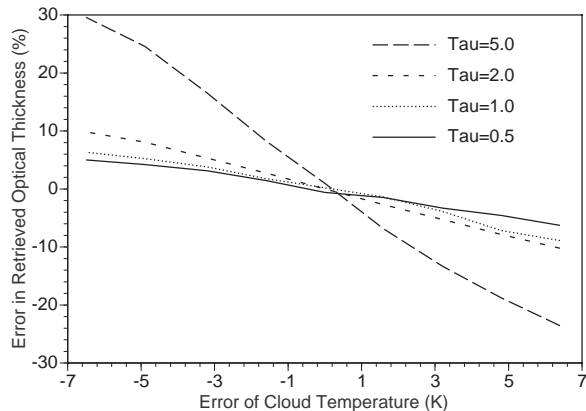

Fig. 6: Errors in retrieved optical thickness resulting from an error in cloud temperature for four optical thicknesses. The ice cloud has an effective particle size of 25 μm. The actual cloud temperature is assumed to be 223.3 K, but varies from 229.7 to 216.8 K.

Figure 7 shows the relationship between the retrieved effective particle size and the cloud temperature error. Different cloud temperatures result in different brightness temperature slopes, and thus lead to effective particle size retrieval errors. The error is within ±15% if the cloud temperature error is within ±5 K.
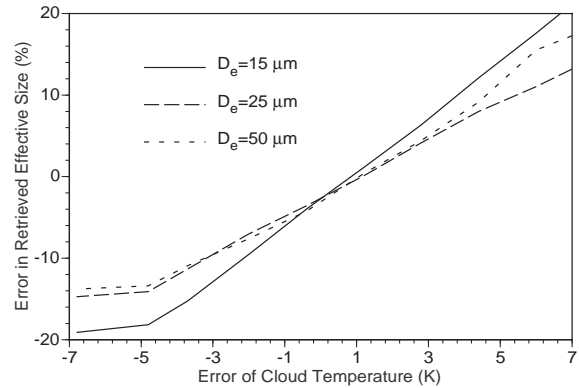

Fig. 7: Errors in retrieved effective size to the error of cloud temperature for 3 effective particle sizes. The ice cloud has an optical thickness of 1.

Figure 8 shows the error in retrieved optical thickness as a function of surface skin temperature error. An error in the surface skin temperature has a pronounced influence on the retrieval of optical thickness if the cloud is optically thin, because the upwelling radiation is primarily from the surface, with some modest attenuation by the atmosphere and cloud. For very thick clouds, an error in the surface skin temperature has little influence on the retrieved optical thickness.
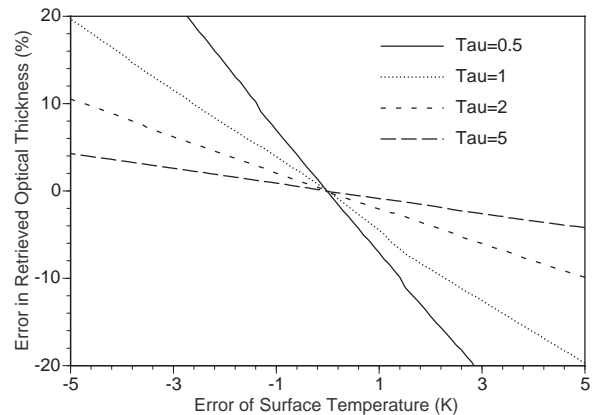

Figure 8. Errors in retrieved optical thickness resulting from an error in surface skin temperature for four cloud optical thicknesses. The ice cloud has an effective particle size of 25 μm and is located at an altitude of 10 km.

From figure 8, it can be seen that if the retrieval accuracy of optical thickness is to be better than 10%, the surface skin temperature error should be less than ±2.5 K. Figure 9 shows the dependence of the retrieved error in effective particle size on the error in surface skin temperature. Compared to the results in figure 8, an error in surface skin temperature (Fig. 9) has less influence on the effective particle size than on the optical thickness, because the variation of the surface skin temperature does not change as much with the slope of brightness temperature between 790–960cm^{-1}. If the error of surface skin temperature

is within ± 2.5 K, the error of retrieved effective particle size will be within $\pm 5\%$.
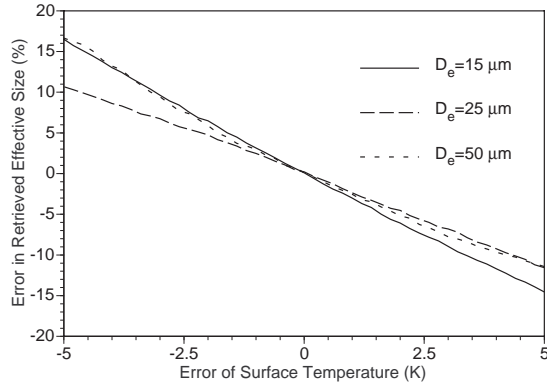

Fig. 9: Errors in retrieved effective size caused by an error in surface skin temperature for three effective particle sizes. The cloud optical thickness is constant at 1, and the cloud altitude is 10 km.

In a subsequent paper we will investigate the sensitivity of the brightness temperature to different regional average atmospheric profiles by calculating the brightness temperature difference between clear-sky and cloudy radiance, defined as the cloud forcing. The variation of cloud forcing will be examined to see IR spectra still contains sufficient information for the simultaneous retrieval of properties of ice clouds.

4. ICE CLOUD MICROPHYSICAL OPTICAL PROPERTIES RETRIEVAL

First, the clear-sky atmospheric optical thickness profile is calculated with the LBL radiative transfer code. Given an ice cloud's height and temperature, a series of spectral radiances are simulated using DISORT for a range of cloud effective particle sizes and optical thicknesses, and additional pre-calculated cloud optical properties discussed in the above sections. By matching the slope of brightness temperature in the 790–960 cm^{-1} band to the observed spectrum, the effective particle size of the ice cloud D_e can be estimated (note that, at this initial stage, a first-guess optical thickness is required). Then the optical thickness is derived by comparing the observed spectrum to the simulations in 1100–1250 cm^{-1} band with the values of D_e determined in the previous step.

The final particle size and optical thickness are obtained by iteration until the differences are minimized between the observed and simulated IR spectrum. A best-fit value is reached when the difference (variance) between the observed and simulated IR spectrum within the two bands is minimal.

In Fig. 10, we illustrate the process of matching the simulated and observed HIS brightness temperatures by varying the cloud properties in the simulations. The left panel of Fig.10 shows comparisons of the observed HIS spectrum (solid black curve) with simulated brightness temperatures for a number of trial effective particle sizes D_e=35, 45, and 60 µm and a first-guess optical thickness Tau=1.43, within the 760–1000 cm^{-1} band.
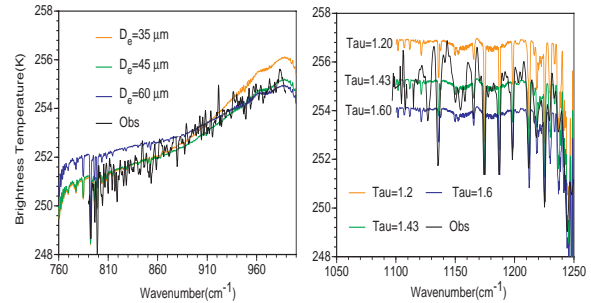

Fig. 10: The simultaneous retrieval of the effective size and optical thickness of ice clouds from HIS spectra. (a) Brightness temperature versus particle size assuming Tau=1.43. (b) Brightness temperature versus optical thickness assuming D_e=45 µm. Date: 23 May 1998, 00:17:01 UT. The surface skin temperature is 267.6 K, and the cloud altitude is 7.0 km.

The right panel of Fig.10 shows brightness temperatures for the best-matched effective particle size D_e=45.0 µm (as determined from the previous step as illustrated in left panel of Fig.10) with trial optical thickness values Tau=1.2, 1.43, and 1.6 within the 1100–1250 cm^{-1} band). The slope is derived from a fitted line between 790–960 cm^{-1}, and then the slope is used for retrieving effective cloud particle size. The resultant values of the effective particle size and optical thickness in this case are therefore 45 µm and 1.43 respectively.

In a following paper we will present more ice clouds properties retrievals from other filed experiments.

5. SUMMRY

Within the 750–1000 cm^{-1} spectral region, the slope of brightness temperature is sensitive to ice crystal effective particle size, particularly for small particles. At wavenumbers between 1100 and 1250 cm^{-1}, the spectrum is more sensitive to the optical thickness than to particle size. Thus, using the terrestrial window information within the 750–1250 cm^{-1} spectral band, we can infer the optical thickness and effective particle size for ice clouds simultaneously.

While the error analysis shows that the uncertainty of the retrieved optical thickness and effective particle size exhibits a small variation. The error for retrieving particle size in conjunction with an uncertainty of 5 K in cloud temperature, or a surface temperature uncertainty of 2.5 K, is less than 15%. The corresponding error in the uncertainty of optical thickness is within 5-20%, depending on the value of cloud optical thickness.

The maximum effective particle size that may be retrieved with the present approach (i.e., an upper limit) is 80 µm with an uncertainty of approximately 10

μm at D_e=80 μm, and about 2 μm uncertainty at D_e=10 μm. The maximum retrievable optical thickness is approximately 8 with an uncertainty of 1. For the case of optical thickness 1, the uncertainty decreases to less than 0.1.

The applicability of the technique is demonstrated using the aircraft–based HIS data from the SUCCESS in 1996.

ACKNOWLEDGEMENT

REFERENCES

Arnott, W. P., Y. Y. Dong, and J. Hallett, 1995: Extinction efficiency in the infrared (2-18 μm) of laboratory ice clouds: observations of scattering minimum in the Christiansen bands of ice, *Appl. Opt.* , vol. 34, pp.541–551.

Chou, M.D. and L. Kouvaris, 1986: Monochromatic calculations of atmospheric radiative transfer due to molecular line absorption, *J. Geophys. Res.*,vol. 91, pp.4047-4055.

Hu Y. X., B. Wielicki, B. Lin, G. Gibson, S. C. Tsay, K. Stamnes, and T. Wong, 2000: Delta-fit: A fast and accurate treatment of particle scattering phase functions with weighted singular-value decomposition least-square fitting, J. Quant. Spectrosc. Radiat. Transfer, vol. 65, pp.681-690.

Huang H. L., W. L. Smith, J. Li, P. Antonelli, X. Wu, R. O. Knuteson, B. Huang, and B. J. Osborne, 2003: Minimum local emissivity variance retrieval of cloud altitude and effective spectral emissivity simulation and initial verification, accepted by *J. Appl. Meteo.*

Kielkopf, J. F., 1973: New Approximation to the Voigt Function with application to spectral line profiles, *J. Opt. Sci. Am.*, vol. 63, pp.987–995.

Revercomb, H.E., H. Buijs, H.B. Howell, D.D. Laporte, W.L. Smith, and L.A. Sromovsky, 1988: Radiometric calibration of IR fourier transform spectrometers: solution to a problem with the High-resolution Interferometer Sounder (HIS). Appl. Opt., 27, pp. 3210-3218.

Rothman, L. S., C. P. Rinsland, A. Goldman et al., 1998: The HITRAN Molecular Spectroscopic Database and HAWKS (HITRAN Atmospheric Workstation): 1996 Edition, *J. Quant. Spectrosc. Radiat. Transfer*, vol. 60, pp. 665–710.

Stamnes, K., S. C. Tsay, W. Wiscombe and K. Jayaweera, 1988: A numerically stable algorithm for discrete-ordinate-method radiative transfer in multiple scattering and emitting layered media, *Appl. Opt.*, vol. 27, pp.2502–2509.

Tobin, D. C., F. A. Best, S. A. Clough, R. G. Dedecker, R. G. Ellingson, R. K. Garcia, H. B. Howell, R. O. Knuteson, E. J. Mlawer, H. E. Revercomb, J. J. Short, P. F. W. van Delst, and V. P. Walden, 1999: Downwelling spectral radiance observations at the SHEBA ice station: Water vapor continuum measurements from 17–26 μm, *J. Geophys. Res.*, vol. 104, pp. 2081–2092.

Wiscombe, W. J., 1980: Improved Mie scattering algorithms, *Appl. Opt.*, vol.*19*, pp.1505–1509.

Wylie, D. P. and W. P. Menzel, 1999: Eight years of global high cloud statistics using HIRS, *J. Climate,* vol. 12, pp.170–184.

Yang, P., B. C. Gao, B. A. Baum, Y. X. Hu, W. J. Wiscombe, S. C. Tsay, D. M. Winker, and S. L. Nasiri, 2001: Radiative properties of cirrus clouds in the infrared (8–13 μm) spectral region, *J. Quant. Spectrosc. Radiat. Transfer*, vol.70, pp. 473–504.

Yang, P., and K. N. Liou, 1996: Finite-difference time domain method for light scattering by small ice crystals in three-dimensional space, *J. Opt. Soc. Amer.,* vol. A13, pp. 2072-2085.

Yang, P., K. N. Liou and W. P. Arnott, 1997: Extinction efficiency and single-scatttering albedo for laboratory and natural cirrus clouds, *J. Geophys. Res.*, vol. 103, pp. 825–835.